

Determination of the Si Young's modulus between room and melt temperature using the impulse excitation technique

Akhilesh K. Swarnakar¹, Omer Van der Biest¹, and Jan Vanhellemont^{*,2}

¹ Department of Metallurgy and Materials Engineering (MTM), KU Leuven, Belgium

² Department of Solid State Sciences, Ghent University, Belgium

Received 22 April 2013, revised 6 June 2013, accepted 1 November 2013

Published online 5 December 2013

Keywords Si, Young's modulus, elastic compliances, impulse excitation technique

* Corresponding author: e-mail jan.vanhellemont@ugent.be, Phone: +32-499-593857, Fax: +32-9-2644996

Stress induced by the thermal gradients near the melt-solid interface affects the intrinsic point defect properties and the quality of single crystal Si grown from a melt. Also during device processing, stress in the Si substrate influences point defect behavior during thermal treatments. To be able to simulate and control the stress distribution one needs to know the elastic constants of single crystal Si at high temperatures. In the present study, the vibrational properties of single crystal Si samples are studied between room and melt temperature using the impulse excitation technique.

From the measurements, the temperature dependent Young's moduli $E_{\langle ijk \rangle}$ of moderately doped Czochralski-grown Si samples are extracted in the $\langle 100 \rangle$, $\langle 110 \rangle$ and $\langle 111 \rangle$ crystallographic directions. Close to the melt temperature, very high Young's moduli values between 110 and 160 GPa are obtained, depending on the crystallographic direction. Empiric expressions are derived for the temperature dependence of $E_{\langle 100 \rangle}$, $E_{\langle 110 \rangle}$ and $E_{\langle 111 \rangle}$ and of the elastic compliances s_{11} and $s_{12} + s_{44}/2$, useful for application in process simulation.

© 2013 WILEY-VCH Verlag GmbH & Co. KGaA, Weinheim

1 Introduction Mechanical and thermal stresses play an important role in many of the processes used to produce electronic devices. For example, Si single crystals are grown from a melt using the Czochralski or floating zone technique. Near the melt/solid interface high thermal stresses develop that in the worst case can lead to dislocation formation and the loss of the crystal. As recently demonstrated, stress even has an important impact on the process window to pull so called perfect crystals [1,2]. Also during device fabrication, processing steps like thermal treatments, growth of thin films, ion implantation lead to the development of stress in the substrate which will be determined by the temperature dependent elastic properties of Si [3,4]. It is therefore surprising that despite the huge research effort during the last half century to develop the Si based electronics industry, no data can be found in the

literature on the Young's modulus $E_{\langle ijk \rangle}$ of Si in the $\langle ijk \rangle$ direction above 1000 °C.

More than 10 years ago, Ono et al. used the flexural vibration method to determine $E_{\langle ijk \rangle}$ of B doped Si up to a temperature of 1000 °C and showed that it remained surprisingly high in contrast with previous reports [5]. They also showed that between room temperature and 1000 °C, $E_{\langle ijk \rangle}$ shows no dependence on B concentration for concentrations up to $8.5 \times 10^{18} \text{ cm}^{-3}$. A few years later Kury et al. [6] re-calibrated the pioneering experimental data of Burenkov et al. of the early 1970's [7–9], and derived polynomial expressions for the dependence on temperature between room temperature and 1000 °C of the bi-axial Young's modulus $E_{\langle ijk \rangle}/(1 - \nu)$, with ν the Poisson ratio. The results were similar to those of Ono et al., revealing

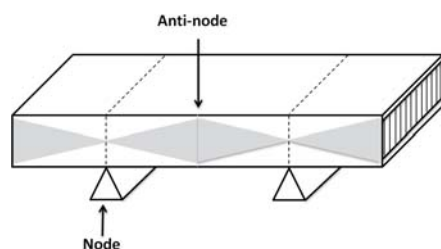


Figure 1 Flexural resonant vibration modes in a rectangular plate. Ideally the specimen is suspended at the nodes to minimize damping.

a limited dependence on temperature of Young's modulus up to 1000 °C.

In the present paper, the impulse excitation technique (IET) [10] is used to determine the temperature dependence of $E_{\langle 100 \rangle}$, $E_{\langle 110 \rangle}$ and $E_{\langle 111 \rangle}$ up to the Si melt temperature. A similar set-up is used as was used by Ono et al. [5] but equipped with a specimen chamber and specimen suspension system allowing heating samples up to 1500 °C. From the experimental results, empiric expressions are derived for the temperature dependent elastic compliances s_{11} and $s_{12} + s_{44}/2$. These allow calculating the Si temperature dependent mechanical properties to be used in device and process simulations.

The impulse excitation technique (IET) measures the fundamental resonant frequency (f_r) of a specimen of suitable geometry as illustrated in Figs. 1 and 2, by exciting it mechanically with an impulse tool. The resonance frequencies are characteristic for the test object, as they are related to its stiffness, mass and geometry. The amplitude decay of a free vibration can be related to the internal friction, i.e. dissipation of the vibration energy or damping. Measurement of the resonance frequency allows the calculation of the Young's modulus (E).

2 The impulse excitation technique (IET) The method of measurement relies on inducing a transitory vibration in the sample, recording the vibration (amplitude as a function of time) and extracting the relevant resonance frequencies (f_r). Specimen supports, impulse locations, and signal pick-up points are selected to induce and measure specific modes of the transient vibrations (Fig. 1). A transducer (for example, microphone) senses the resulting mechanical vibrations of the specimen and transforms them into electric signals. The transient signals are analyzed and the fundamental resonant frequency is isolated and measured by the signal analyzer, which provides a numerical reading that is (or is proportional to) either the frequency or the period of the specimen vibration. The appropriate fundamental resonant frequencies, dimensions and mass of the specimen are used to calculate $E_{\langle ijk \rangle}$.

According to ASTM - C1259-08 [11], in the case of isotropic rectangular samples, the elastic modulus of the

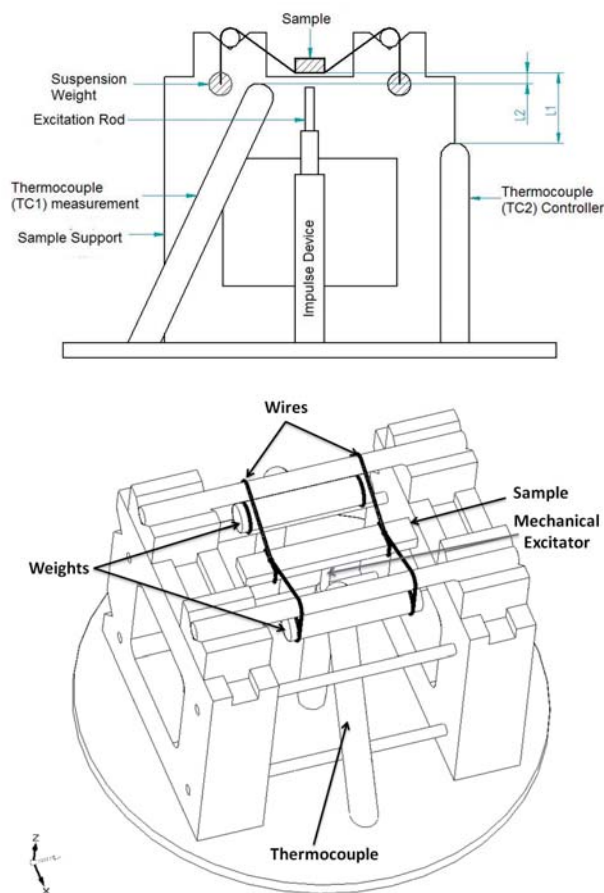


Figure 2 Schematic diagrams of the IET setup (top) and of the specimen suspended by carbon wires inside the furnace (bottom) [12].

material can be calculated as

$$E_{\langle ijk \rangle} = 0.9465 \frac{m f_r^2}{b} \left(\frac{L}{t} \right)^3 T_1, \quad (1)$$

where $E_{\langle ijk \rangle}$ is the Young's modulus (in Pa), f_r the resonance frequency in flexural mode (in Hz), m the mass of the sample (in g), T_1 a correction factor for the fundamental flexural mode to account for finite thickness of the bar, Poissons ratio, etc.. L , b and t are the length along the $\langle ijk \rangle$ direction, the width and the thickness of the sample (in mm), respectively.

3 Relations between the elastic parameters of crystals with the diamond structure

3.1 Relation between Young's modulus and the elastic compliances The Young's modulus for a crystallographic direction $\langle ijk \rangle$ can also be expressed as function

of the elastic compliances s_{11} , s_{12} and s_{44} [13–17] as

$$\frac{1}{E_{\langle ijk \rangle}} = s_{11} - 2(s_{11} - s_{12} - \frac{1}{2}s_{44})(l_1^2 l_2^2 + l_2^2 l_3^2 + l_1^2 l_3^2), \quad (2)$$

with l_i , the direction cosines for the given direction.

And for the directions studied in the present study

$$\begin{aligned} \frac{1}{E_{\langle 100 \rangle}} &= s_{11} \\ \frac{1}{E_{\langle 110 \rangle}} &= s_{11} - \frac{1}{2} \left(s_{11} - s_{12} - \frac{1}{2}s_{44} \right) \\ \frac{1}{E_{\langle 111 \rangle}} &= s_{11} - \frac{2}{3} \left(s_{11} - s_{12} - \frac{1}{2}s_{44} \right). \end{aligned} \quad (3)$$

3.2 Relation between stiffness coefficients and elastic compliances The relationship between the elastic stiffnesses and compliances is given by [14]

$$\begin{aligned} s_{11} &= (c_{11} + c_{12})/(c_{11} - c_{12})(c_{11} + 2c_{12}) \\ s_{12} &= -c_{12}/(c_{11} - c_{12})(c_{11} + 2c_{12}) \\ s_{44} &= 1/c_{44}. \end{aligned} \quad (4)$$

Based on invariance requirements for the elastic strain energy in diamond structure crystals, Keating [20] derived following relation between the stiffness coefficients c_{ij}

$$2c_{44}(c_{11} + c_{12}) = (c_{11} - c_{12})(c_{11} + 3c_{12}). \quad (5)$$

4 Materials and experimental conditions As-grown, B doped Si material with a resistivity of 7–12 $\Omega \times \text{cm}$ and an interstitial oxygen content of 23–25 ppma (old ASTM) is used in this study. Specimens are prepared by cutting the as-grown crystals or by cleaving the wafers. The dimensions of the specimens are about $45 \times 7 \times 2 \text{ mm}^3$ ($L \times b \times t$). To remove the mechanical damage, the samples are mirror etched. Before the measurement the geometry and weight of each sample is measured accurately.

A uniform rectangular bar can have various natural modes of vibration like longitudinal, torsional or flexural, depending on suspension of the sample (free or clamped). In the present experiments, samples are suspended in flexural mode inside the furnace using carbon wires at the bending nodes, which have minimum motions at these points as illustrated in Fig. 1. For a rectangular plate specimen, the nodes are located at a distance of about $0.224 \times L$ from the specimen edge.

The high temperature IET measurements are performed using a IMCE HTVP 1750 IET set-up equipped with automated impulse excitation and vibration detection devices. The samples are suspended with carbon wires holding the sample at its vibration nodes using weights (Fig. 2). Mechanical excitation is performed by periodically (minutes scale) hitting the sample from below near the center with a ceramic rod. This is different from the

Table 1 Coefficients of (6), with T in $^\circ\text{C}$ and $E_{\langle ijk \rangle}$ in GPa, obtained from the best fits to the experimental data as shown in Fig. 3. In the last column also the goodness of the fit is given by the coefficient of determination R^2 .

$\langle ijk \rangle$	A_0	A_1 ($\times 10^{-3}$)	A_2 ($\times 10^{-6}$)	R^2
$\langle 100 \rangle$	127.5 ± 0.1	-6.3 ± 0.3	-4.4 ± 0.2	0.947
$\langle 110 \rangle$	161.26 ± 0.03	-7.00 ± 0.09	-5.60 ± 0.06	0.997
$\langle 111 \rangle$	181.8 ± 0.1	-7.9 ± 0.3	-5.9 ± 0.2	0.972

approach of Ono et al. [5] who used an alternating current electric field to excite the samples. The acoustic wave generated in the sample is guided to a microphone outside the furnace using a alumina tube. The samples are heated in argon atmosphere from room temperature up to about 1400 $^\circ\text{C}$ using heating rates of 5 or 7 $^\circ\text{C}/\text{min}$. A more detailed description of the equipment and the measuring technique can be found in literature [10, 12].

5 Results and discussion The measurement results obtained on three samples for each crystallographic direction, are shown in Fig. 3 illustrating that the measurements are quite reproducible with a variation of only a few % between samples. As for each sample a measurement is performed every few degrees, the measurement points form the continuous colored lines that are shown in the figure (no smoothing was performed) illustrating also the stability of the measurement and the very small scatter of the data points during one measurement session which can take up to 8 h. For each direction, one of the samples is measured up to the melt temperature which is visible by the sudden drop in Young's modulus in the figures showing the $\langle 100 \rangle$ and $\langle 111 \rangle$ results. Similar measurements (not shown here) are also performed during cooling to room temperature from the maximum temperature revealing a very similar curve close to the one obtained during the ramp-up of the temperature. This shows that the sample properties are not significantly changed by the temperature ramp-up process.

The observed temperature dependence of the Young's modulus above 800 $^\circ\text{C}$ is smaller than the one reported by Ono et al. (Fig. 5 in [5]) which is probably due to the fact that they used Pt wires to suspend the samples. Above 350 $^\circ\text{C}$, PtSi is formed which is softer than Si and has a melting point around 1225 $^\circ\text{C}$. Due to this an apparent lower Young's modulus is expected. This problem does not arise when using carbon wires as SiC is only formed at very high temperatures. Close to the Si melt temperature (starting from about 1390 $^\circ\text{C}$) there is however also a clear reaction of the carbon wires with the Si sample with considerable consumption of Si. As SiC is harder than Si and has a melting temperature of about 2730 $^\circ\text{C}$, a slight overestimate of the modulus can be expected in this case, close to the Si melt temperature.

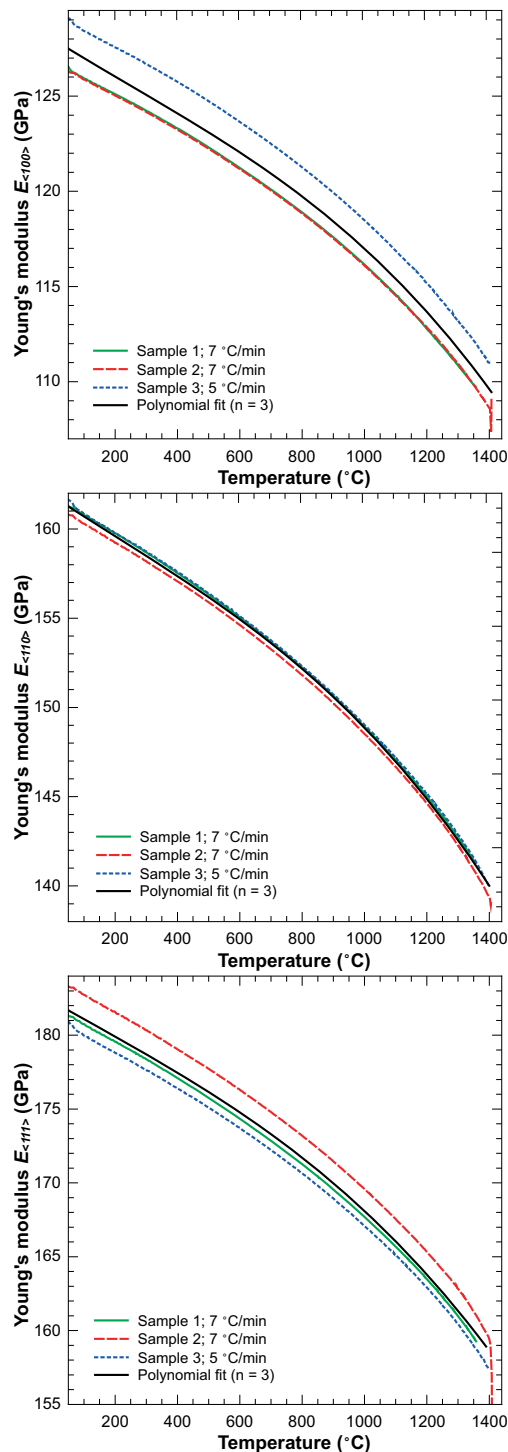


Figure 3 E_{ijk} measured along the $\langle 100 \rangle$ (top), $\langle 110 \rangle$ (middle) and $\langle 111 \rangle$ (bottom) directions on each time three samples. In each figure the best second order polynomial fit to all experimental data, is shown by the full black line. The corresponding coefficients are listed in Table 1.

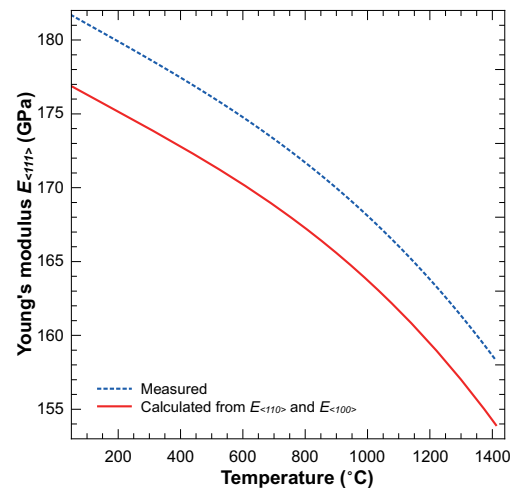


Figure 4 Young's modulus $E_{\langle 111 \rangle}$ can also be calculated from the best fits of $E_{\langle 110 \rangle}$ and $E_{\langle 100 \rangle}$ in Fig. 3 and the result is shown together with the best fit from the bottom figure of Fig. 3 illustrating the good agreement between the calculated and measured result with a difference that is smaller than 3%.

The best fits in Fig. 3 are obtained using a second order polynomial given by

$$E_{ijk} = A_0 + A_1T + A_2T^2. \quad (6)$$

The results of the best fits are shown in Table 1 and Fig. 4.

6 Comparison with previous results

6.1 Room temperature Accurate room temperature values for s_{11} , s_{12} and s_{44} , i.e. 7.68, -2.14 and 12.6 (in $10^{-12}Pa$), respectively, were obtained by Hall [18]. Substitution in Eq. (3) yields $E_{\langle 100 \rangle}$, $E_{\langle 110 \rangle}$ and $E_{\langle 111 \rangle}$ values of 130, 169 and 188 (in GPa), respectively, in excellent agreement with the values of 127, 161 and 182 GPa, obtained in the present study.

6.2 Temperature dependence of E_{ijk} , s_{11} and $s_{12} + s_{44}/2$ Figure 5 shows a comparison of published results with those obtained in the present study. Between room temperature and $1000^\circ C$ there is a good agreement and the differences are within the experimental error. The results of Burenkov were obtained by assuming a Poisson ratio of 0.262 and 0.17 for $E_{\langle 100 \rangle}$ and $E_{\langle 111 \rangle}$, respectively.

The somewhat different shape of the lines corresponding with the Ono et al. data is due to the fact that they fitted an exponential dependence to the experimental data points which was probably not the best choice. A polynomial fit to their data would be much closer to the other results.

The results obtained in the present study show that the Young's moduli continue to decrease smoothly with increasing temperature above $1000^\circ C$ and this up to the melt temperature. Near melt temperature a very high modulus remains which is well above 100 GPa for the three main crystallographic directions. This is more than three

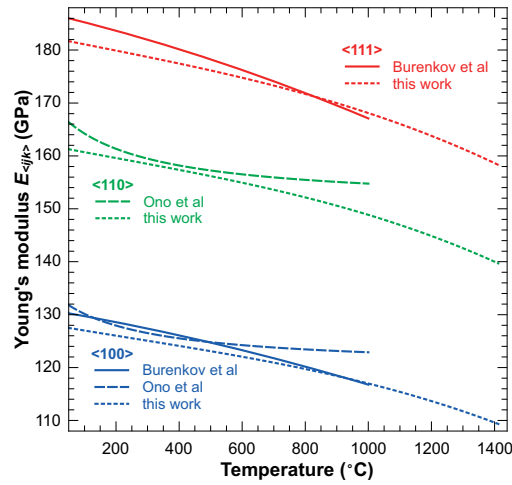


Figure 5 Comparison between the results of Ono et al. [5] and of Burenkov et al. [6–9] and of the present study.

Table 2 Coefficients of (7), with T in $^{\circ}\text{C}$ and s_{ij} in 10^{-12} Pa^{-1} , obtained from the best fits to the curves in Fig. 6. In both cases, the coefficient of determination R^2 is larger than 0.998

s_{ij}	B_0	B_1 ($\times 10^{-4}$)	B_2 ($\times 10^{-7}$)
s_{11}	7.864 ± 0.001	2.74 ± 0.04	4.27 ± 0.03
$s_{12} + s_{44}/2$	4.5666 ± 0.0005	1.09 ± 0.02	2.18 ± 0.01

orders of magnitude larger than what was estimated by Wijaranakula (Fig. 3 in [19]) based on the von Mises yield criterion for plastic deformation. This estimate was however most probably wrong and a strong underestimation as it was based on the extrapolation of yield stresses determined experimentally on basis of plastic deformation by dislocation formation at low temperatures to a yield stress near melt temperature. The yield stress (leading to dislocation formation) is however always much lower than the elastic moduli for perfect, dislocation free, material.

Due to this high value, the thermal stress near the melt-solid interface in Si crystals growing from a melt is of the order of tens of MPa and increases with increasing crystal diameter thus posing a serious challenge for the development of 450 mm crystals and for thermal processing of the 450 mm wafers.

Based on the empirical expressions derived for the temperature dependence of $E_{\langle ij \rangle}$ given in Eq. (6) and in Table 1 and taking into account the relation between the Young's modulus and the compliances given in Eq. (3), one can calculate the curves in Fig. 6 that are well described by

$$s_{ij} = B_0 + B_1 T + B_2 T^2, \quad (7)$$

with B_i listed in Table 2.

6.3 Comparison with published results on Ge

Already in 1971, Burenkov et al. [21] published results on

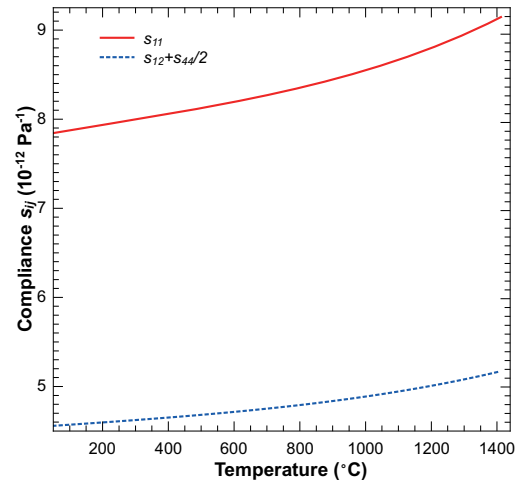


Figure 6 Compliances calculated using Eq. (3) with the coefficients obtained from the best fit for $E_{\langle 110 \rangle}$ and $E_{\langle 100 \rangle}$ listed in Table 1.

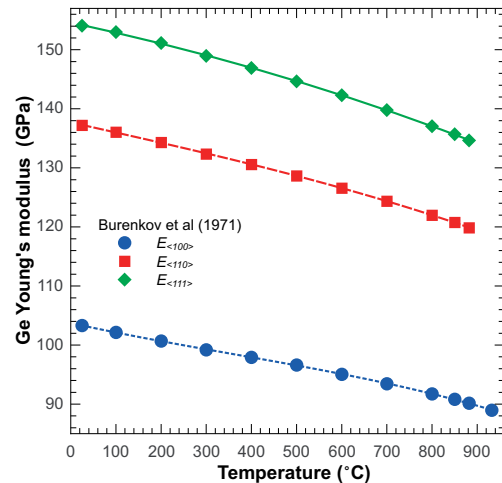


Figure 7 Dependence of Young moduli of Ge on temperature as obtained by Burenkov et al. [21]. The lines are second order polynomial fits using Eq. (6) and the obtained coefficients are listed in Table 3.

the dependence of the mechanical properties of Ge up to the melt temperature which are shown in Fig. 7. Similar as for Si, the Young modulus decreases smoothly up to T_m and remains remarkably high. It is known that many properties of Ge show a similar dependence on temperature as in Si [22]. This is in particular clear when plotting the data as function of the temperature (in K) normalized with respect to the melt temperature. Figure 8 illustrates this by showing the normalized $E_{\langle 111 \rangle}$ Young moduli of Si (this work and Burenkov data as processed by Kury et al. [6]) and Ge (Burenkov et al. experimental data [21] and second order polynomial fit) as a function of the normalized temperature. The Young moduli are normalized to the value at

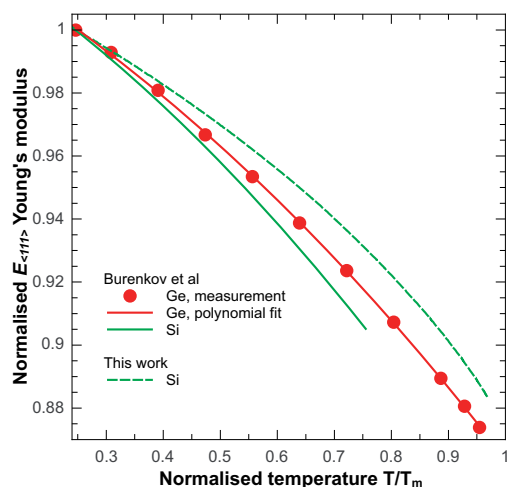


Figure 8 Normalized E_{111} Young modulus versus normalized temperature T/T_m for Si and Ge. The data for Ge are based on the results of Burenkov et al. [21].

Table 3 Coefficients of (6), with T in $^{\circ}\text{C}$ and $E_{\langle ijk \rangle}$ in GPa, obtained for Ge using the experimental data of Burenkov et al. [21]. In all cases the coefficient of determination R^2 is larger than 0.999.

Direction	A_0	A_1 ($\times 10^{-2}$)	A_2 ($\times 10^{-6}$)
$\langle 100 \rangle$	103.4 ± 0.2	-1.21 ± 0.07	-3.3 ± 0.7
$\langle 110 \rangle$	137.58 ± 0.07	-1.52 ± 0.04	-5.4 ± 0.4
$\langle 111 \rangle$	154.57 ± 0.07	-1.62 ± 0.04	-7.2 ± 0.4

$T/T_m = 0.246281$ which corresponds with room temperature (298 K) for Ge. It is obvious that the dependence of Young modulus of Si and Ge on temperature is very similar. This has of course implications for thermal processing of device structures containing active Ge layers on a Si substrate. At the same processing temperature the decrease of the Young modulus of the Ge film is always considerably larger than that of the Si substrate.

Dedicated Ge specimens have been prepared to perform Young modulus measurements up to the melt temperature using the impulse excitation technique as for Si and detailed analyses and comparison with the historical Burenkov data for Ge will be published elsewhere.

7 Conclusions The Young's moduli of mono-crystalline Czochralski grown Si were measured between room temperature and melt temperature for $\langle 100 \rangle$, $\langle 110 \rangle$ and $\langle 111 \rangle$ crystallographic directions. For the first time measurements were also performed above 1000 $^{\circ}\text{C}$ and the obtained $E_{\langle ijk \rangle}$ values are surprisingly high and remain well above 100 GPa up to the melt temperature. The results show that thermal stress levels not only in Si crystals growing from a melt but also in Si wafers during high

temperature processing steps will be higher than assumed so far.

Comparison with published data for Ge shows that the temperature dependence of the elastic constants of both materials is very similar, in particular when expressed as function of the temperature normalized with respect to the melt temperature.

Acknowledgements Siltronic AG and ON Semiconductor are acknowledged for supplying the samples for the IET measurements.

References

- [1] J. Vanhellemont, J. Appl. Phys. **110**, 063519, 129903 (2011).
- [2] J. Vanhellemont, E. Kamiyama, and K. Sueoka, ECS J. Solid State Sci. Technol. **2**, P166 (2013).
- [3] S. M. Hu, J. Appl. Phys. **70**, R53 (1991).
- [4] J. Vanhellemont, Electrochem. Soc. Proc. **98-1**, 997 (1998).
- [5] N. Ono, K. Kitamura, K. Nakajima and Y. Shimanuki, Jpn. J. Appl. Phys. **39**, 368 (2000).
- [6] P. Kury and M. Horn-von Hoegen, Rev. Sci. Instrum. **75**, 1357 (2004).
- [7] S. P. Nikanorov, Y. A. Burenkov and A. V. Stepanov, Sov. Phys. Solid State **13**, 2516 (1972).
- [8] Y. A. Burenkov and S. P. Nikanorov, Sov. Phys. Solid State **16**, 963 (1974).
- [9] Y. A. Burenkov and S. P. Nikanorov, Solid State Phys. **26**, 3224 (1984) (in Russian).
- [10] G. Roebben, B. Bollen, A. Brebels, J. Van Humbeeck, and O. Van der Biest, Rev. Sci. Instrum. **68**, 4511 (1997).
- [11] ASTM C1259 08, Standard Test Method for dynamic Young's modulus, shear modulus, and Poisson's ratio for advanced ceramics by impulse excitation of vibration.
- [12] A. K. Swarnakar, Ph.D. dissertation, KU Leuven (2012).
- [13] J. J. Wortman and R. A. Evans, J. Appl. Phys. **36**, 153 (1965).
- [14] W. A. Brantley, J. Appl. Phys. **44**, 534 (1973).
- [15] J. F. Nye, Physical Properties of Crystals: Their Representation by Tensors and Matrices (Oxford Univ. Press, Oxford, U.K., 1985).
- [16] Properties of Silicon, EMIS Data Rev. Ser., No. 4 (INSPEC, London, 1988), p. 14.
- [17] M. A. Hopcroft, W. D. Nix, and T. W. Kenny, J. Microelectromech. Syst. **19**, 229 (2010).
- [18] J. J. Hall, Phys. Rev. **161**, 756 (1967).
- [19] W. Wijaranakula, J. Electrochem. Soc. **140**, 3306 (1993).
- [20] P. N. Keating, Phys. Rev. **145**, 637 (1966).
- [21] Yu. A. Burenkov, S. P. Nikanorov, and A. V. Stepanov, Soviet Phys. - Solid State **12**, 1940 (1971).
- [22] J. Vanhellemont and E. Simoen, J. Electrochem. Soc. **154**, H572 (2007).